

ARTICLE

Theoretical Study of Reaction Mechanism of 1-Propenyl Radical with NO

Xue-li Cheng^{a*}, Yan-yun Zhao^{a,b}, Feng Li^c, Ren-tao Wu^a*a.* Department of Chemistry, Taishan University, Tai'an 271021, China*b.* Department of Chemistry, Qufu Normal University, Qufu 273165, China*c.* Department of Physics, Taishan University, Tai'an 271021, China

(Dated: Received on August 6, 2007; Accepted on October 14, 2007)

The reaction system of 1-propenyl radical with NO is an ideal model for studying the intermolecular and intramolecular reactions of complex organic free radicals containing C=C double bonds. On the basis of the full optimization of all species with the Gaussian 98 package at the B3LYP/6-311++G** level, the reaction mechanism was elucidated extensively using the vibrational mode analysis. There are seven reaction pathways and five sets of small molecule end products: CH₂O+CH₃CN, CH₂CHCN+H₂O, CH₃CHO+HCN, CH₃CHO+HNC, and CH₃CCH+HNO. The channel of C₃H₅·+NO→IM1→TS1→IM2→TS2→IM3→TS3→CH₃CHO+HCN is thermodynamically most favorable.

Key words: Reaction mechanism, 1-Propenyl radical, NO, Vibrational mode analysis

I. INTRODUCTION

NO has a single electron, and is actually a free radical. Moreover, it can be released to the environment during industrial processes, from lightning, from combustion of heavy fuels [1], and from automobile exhaust and cigarette smoke, and it ultimately affects the atmosphere. Because of its unique reactivity of taking part in a series of free radical reactions, NO attracts interest among theoretical physicists and chemists, and reaction mechanisms of a variety of free radicals like CH₃O₂ [2], OBrO [3], CH₃S [4], C₂($\alpha^3\Pi_u$) [5], NCS [6], CH₃ [7,8], H₂ [9], XCO (X=H,F,Cl) [10], and NH(D) [11] with NO have been reported. C₃H₅, which is isomeric with allyl and glyceryl, plays an important role in combustion processes, photochemistry and interstellar chemistry [12,13]. C₃H₅· has three isomers: allyl, 1-propenyl, and 2-propenyl. Experimental studies on the unimolecular dissociation of 2-propenyl radical [14] and the reactions of C₃H₅·+O₂ [15] have been carried out. Recently, the potential energy surfaces of its isomer allyl radical with NO were reported [16,17]. C₃H₅· is an ideal model for studying the intermolecular and intramolecular reactions of complex organic free radicals containing C=C double bonds, so it is necessary to carry out a theoretical investigation to understand its reactivity. In this study, 1-propenyl radical CH₃CH=CH· is selected and the reaction mechanism of this radical with NO is elucidated.

II. COMPUTATION METHODS

The Gaussian 98 program package [18] was employed to fully optimize all species involved with the reaction

of C₃H₅·+NO at the B3LYP/6-311++G** level. A B3LYP method, namely Becke's three-parameter non-local exchange functional [19] with the nonlocal correlation functional of Lee *et al.* [20], was used throughout the study. It is essential to employ a basis set that possesses sufficient diffuseness to obtain reliable properties for non-covalent interaction. Subsequently, connections of the transition states and products were confirmed by IRC calculations [21-23]. The same procedure in our previous work [24] was used to elucidate the reaction mechanism.

III. RESULTS AND DISCUSSION

1-Propenyl radical has two geometric isomers, specifically, *cis*- and *trans*-CH₃CH=CH·. The *trans*-form, whose internal energy is lower than the maleinoid form by 1.82 kJ/mol, is more stable. Since there is a single p electron on the N atom of NO, in fact NO is also a free radical, so the N atom can combine with C1 atoms of 1-propenyl radicals via barrierless processes, producing three intermediates (IM1, IMa, and IMb). The optimized geometries of the two reactants and three intermediates are shown in Fig.1. The computed relative energies three intermediates compared with the reactants C₃H₅·+NO are -235.71, -206.49, and -229.85 kJ/mol, respectively, so IM1 is energetically the most stable species among these intermediates. Moreover, IM1, IMa, and IMb can be transformed to one another, as shown in Fig.2. The activation energy of converting IMb into IMa via TSab is only 25.20 kJ/mol. Although the potential energy of IMa isomerizing to IM1 via TSb1 is relatively high, *trans*-C₃H₅· can be easily transformed into *cis*-C₃H₅· via TSR with a potential energy of only 28.06 kJ/mol, so *trans*-C₃H₅· can isomerize to *cis*-C₃H₅·, then can react with NO to form IM1. Furthermore, they have similar reactivity, so in this work only IM1 was selected to investigate the de-

*Author to whom correspondence should be addressed. E-mail: ching108@sohu.com

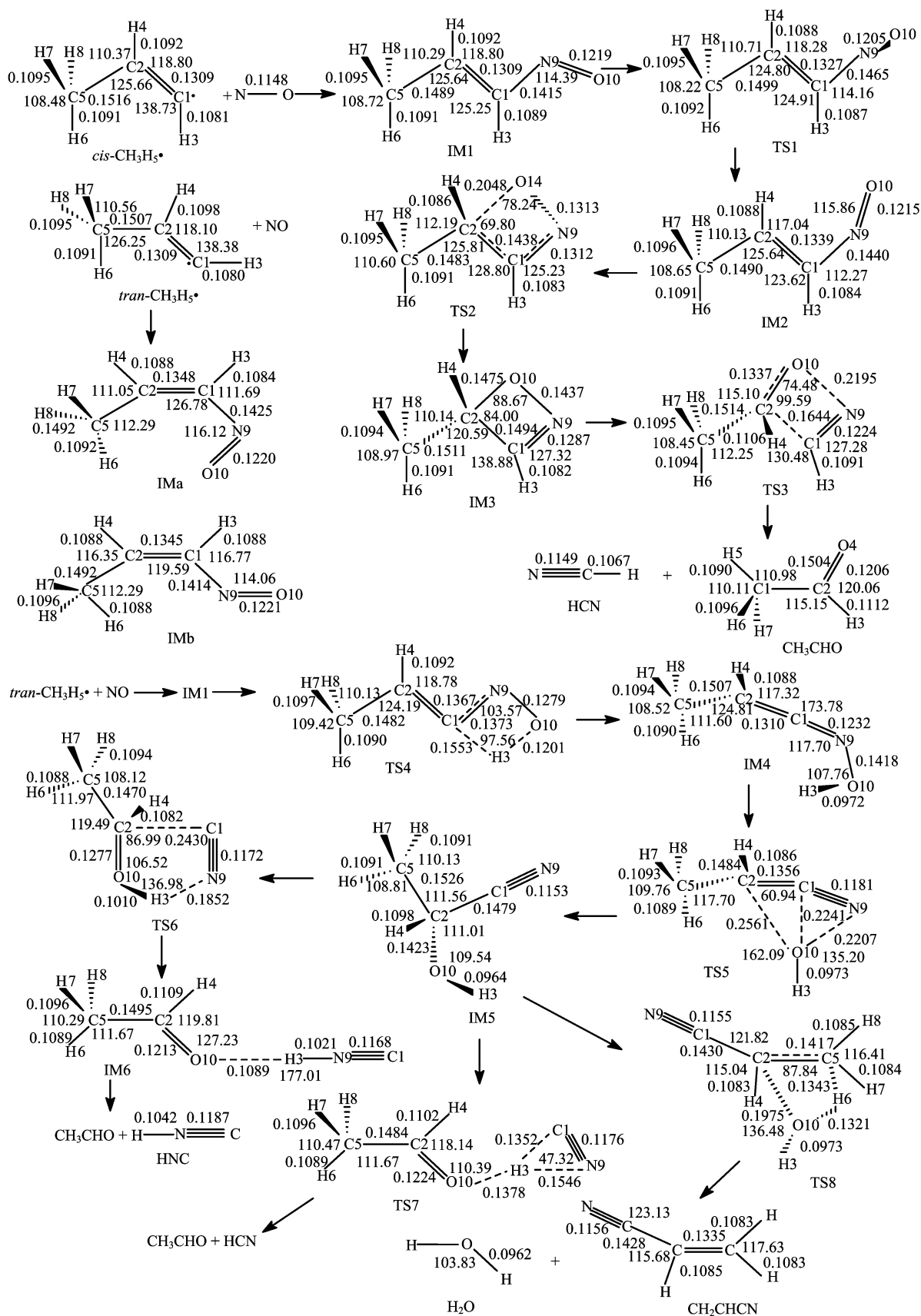


FIG. 1 B3LYP/6-311++G** optimized geometrical parameters for various species of the $C_3H_5 + NO$ reaction system. Bond lengths are in nm and bond angles in $^\circ$. Numbers besides atomic symbols are sequence numbers to distinguish them.

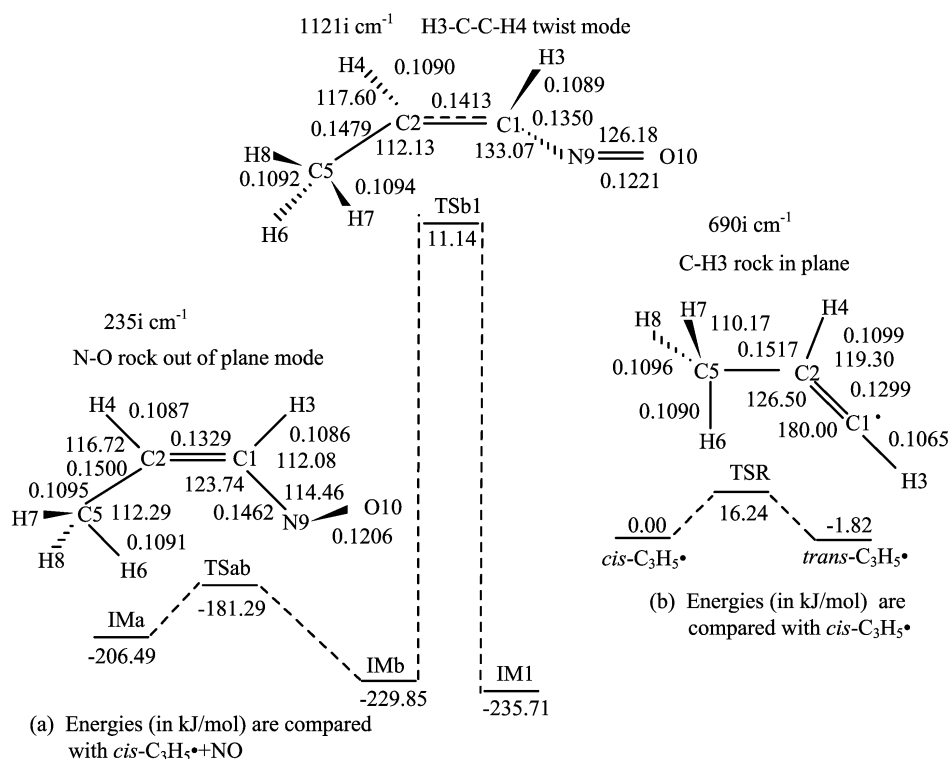


FIG. 2 Sketch maps for the transformation processes among IM1, IMA, IMb, $cis\text{-C}_3\text{H}_5\cdot$, $trans\text{-C}_3\text{H}_5\cdot$, and the geometrical structures, imaginary frequencies for the transition states.

composition pathways.

At the B3LYP/6-311++G** level, all accessible reaction channels were checked, 17 TSs and 5 sets of products. $\text{CH}_2\text{O} + \text{CH}_3\text{CN}$, $\text{CH}_2\text{CHCN} + \text{H}_2\text{O}$, $\text{CH}_3\text{CHO} + \text{HCN}$, $\text{CH}_3\text{CHO} + \text{HNC}$, and $\text{CH}_3\text{CCH} + \text{HNO}$, were found. The optimized geometric parameters of all species regarding the reaction system of $\text{C}_3\text{H}_5\cdot + \text{NO}$ (R) are also exhibited in Fig.1. To elucidate the reaction mechanism, the profile of potential energy surface (PES) is drawn with the relative energies compared with the reactants after zero vibrational point energy correction (ZVPE) and thermal correction (TC). The PES is exhibited in Fig.3.

Vibrational mode analysis can be employed to elucidate reaction mechanisms [24-26]. Analyzing the changes in vibrational modes from reactant to transition states and from transition states to products can explain the direction of the reactions and the degree of chemical reaction. If there is only one imaginary frequency of a transition state, it is always related to the breaking or forming of bonds that are extended. Moreover, the number of imaginary frequencies can confirm whether there is a local minimum or a transition state, so only the first or the lowest frequencies are essential to elucidate the reaction mechanism. Therefore, vibrational mode analysis will be used to investigate the reaction mechanism of $\text{C}_3\text{H}_5\cdot + \text{NO}$. The first frequencies of all species along with their vibrational mode assignment and IR intensity are listed in Table I.

A. Three reaction pathways of $\text{IM1} \rightarrow \text{CH}_3\text{CHO} + \text{HCN}$

IM1 can experience an isomerization process and transform to IM2 via TS1. The only imaginary frequency of TS1 belongs to the N–O rock out of plane mode ($290i\text{ cm}^{-1}$, 0.9173 km/mol), and the shifting O atom erects out of the molecular plane. The potential energy of this channel is only 52.56 kJ/mol and the energy of IM2 is lower than the reactants by 215.56 kJ/mol . Subsequently, O atom bonds to C2 atom via TS2, forming a four-atom-ring IM3. The imaginary frequency of TS2 is assigned to the C2–O stretch mode regarding the newly formed C2–O bond, whose bond distance is 0.2048 nm . Then the C1–C2 bond is extended to 0.1644 nm in TS3, and its stretch mode becomes the imaginary frequency ($1203i\text{ cm}^{-1}$, 42.3824 km/mol); simultaneously the N–O bond is extended to 0.2195 nm . This stretch mode results in the extending of C1–C2 and N–O, finally leading to formation of acetaldehyde CH_3CHO and hydrogen cyanide HCN. The energy barrier of this decomposition process is as high as 204.63 kJ/mol , so it is the speed-determining process of this channel. The relative energy of $\text{CH}_3\text{CHO} + \text{HCN}$ is much lower than the reactants and IM1, and the energies of all TSs are lower than $\text{C}_3\text{H}_5\cdot + \text{NO}$, so this channel is favorable thermodynamically, especially at low temperature range.

Another pathway from IM1 to $\text{CH}_3\text{CHO} + \text{HCN}$ is initiated by a four-atom-ring TS4, by which H3 on

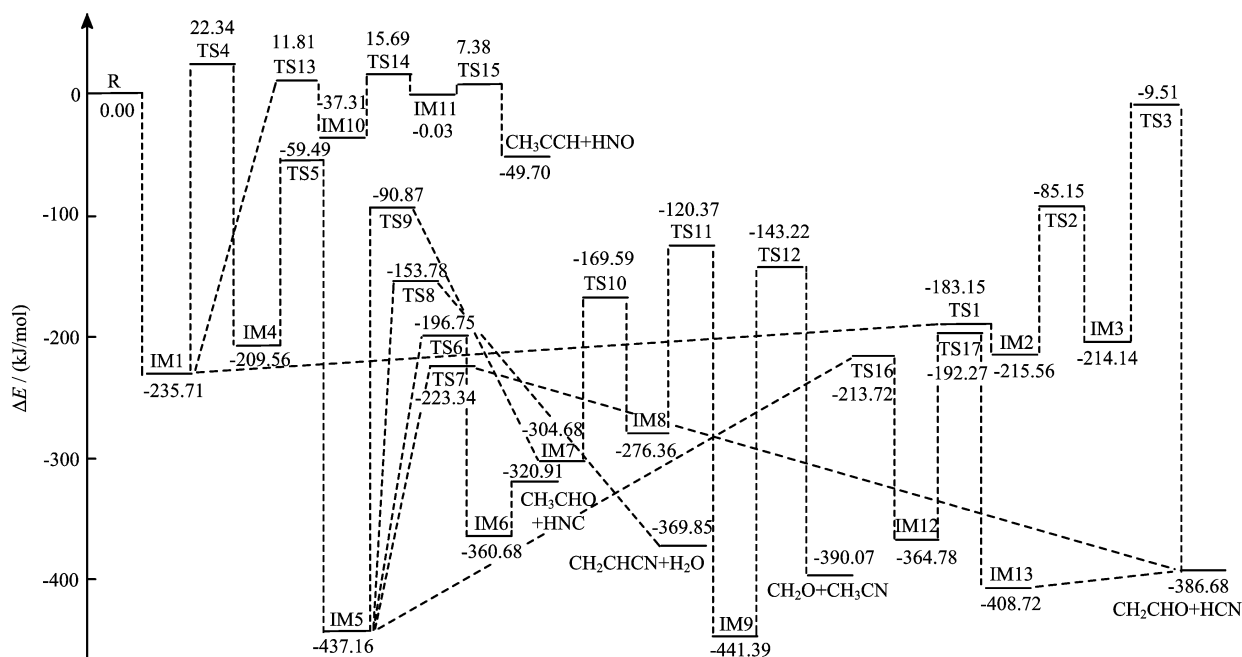


FIG. 3 Overall profile of potential energy surface for the C_3H_5+NO reaction system.

C1 shifts to O atom, leading to IM4 with a hydroxyl group. The imaginary frequency ($1575i\text{ cm}^{-1}$, 179.9820 km/mol) of TS4 is the C–H3 rock in plane mode. The barrier of this process reaches 258.05 kJ/mol , and the energy of TS is higher than the reactants by 22.34 kJ/mol , so it should need extra energy to activate the process and then lead to a variety of products, as shown in Fig.3. The internal energy of IM4 is also relatively high because of its bis(alkylidene) structure. Subsequently the hydroxyl group OH transfers to C2 via TS5, forming IM5. The imaginary frequency of TS5 at $389i\text{ cm}^{-1}$ with an intensity of 65.0909 km/mol is assigned to the N–O–C2 asymmetrical stretch mode. In TS5, the bond distances of O atom to the N, C1, and C2 atom are 0.2207 , 0.2241 , 0.2561 nm , respectively. For IM5, the bis(alkylidene) structure is destroyed and a $C\equiv N$ group forms, so it is very stable, with its energy even lower than some small molecule products. H3 of IM5 can shift to C1 via TS7, and decompose to $CH_3CHO+HCN$. The imaginary frequency of TS7 is assigned to O–H3 rock in plane mode ($581i\text{ cm}^{-1}$, 301.0360 km/mol), which shows that the shifting H3 atom is rocking between the N and C1 atoms.

There is another decomposition channel from IM5 to $CH_3CHO+HCN$. The N atom can link to C2 and the C1–C2 bond rupture through a three-atom-ring TS16, producing IM12. The imaginary frequency of TS16 at $373i\text{ cm}^{-1}$ belongs to the C1–C2–N asymmetrical stretch mode, which exactly shows the formation of C2–N and breaking of the C1–C2 bond. In succession, the $C\equiv N$ group of IM12 will shift to H3 by TS17 to produce IM13. The imaginary frequency of TS17

is the C–H3 and C2–N asymmetrical stretch mode, through which C2–N can break and a new bond C–H3 can form. The $C\equiv N$ group connects to the H3 atom through a weak hydrogen bond (0.2070 nm) instead of capturing the H3 atom because there is not an O–H stretch mode but rather a C–H3 stretch mode. If the hydrogen bonding is destroyed, of course IM13 decomposes to $CH_3CHO+HCN$.

B. Formation of $CH_2CHCN+H_2O$

OH group of IM5 can capture a hydrogen atom from neighboring methyl group, forming $CH_2=CH-C\equiv N$ and H_2O via TS8. The only imaginary frequency of TS8 is the O–H6 stretch mode ($1884i\text{ cm}^{-1}$, 530.1020 km/mol), through which a new O–H6 bond will form and C–H6 bond will break. The energy barrier of this process is 183.38 kJ/mol . Along the reaction coordinate, once the energy barrier of TS4 is surpassed, the five decomposition channels of IM5 will be competitive.

C. Formation of $CH_3CHO+HNC$

There is a reaction pathway from IM5 to acetaldehyde CH_3CHO and isocyanic acid HNC via TS6. In TS6, the only imaginary frequency is assigned to the N–H3 and C1–C2 asymmetrical stretch mode ($357i\text{ cm}^{-1}$, 49.7411 km/mol). The bond lengths of N–H3 and C1–C2 are 0.1852 and 0.2430 nm , respectively. These can engender hydrogen bonding between CH_3CHO and HNC (0.1809 nm), which makes the energy of IM6 lower than that of the end products by 39.77 kJ/mol .

TABLE I First frequencies (in cm^{-1}) and the vibrational mode assignments for all species (intensity is in km/mol)

	Freq.	IR inten.	Mode assignment		Freq.	IR Inten.	Mode assignment
<i>cis</i> -C ₃ H ₅	192	0.7330	Molecule twist	CH ₂ CHCN	239	2.5803	Molecule bend
NO	1980	46.1537	N–O stretch	H ₂ O	1638	58.1244	H–O–H bend
<i>trans</i> -C ₃ H ₅	192	0.0115	Molecule twist	TS9	661i	62.8647	C1–O–C2 asym. stretch
IMa	100	0.5496	Molecule twist	IM7	167	0.2972	Molecule rock i. p.
IMb	140	0.4818	Molecule twist	TS10	567i	59.7349	C1–C2 stretch
IM1	134	0.0113	Molecule rock o. p.	IM8	57	0.2422	Molecule rock i. p.
TS1	290i	0.9173	N–O rock o. p.	TS11	2032i	1066.7039	C1–H3 rock i. p.
IM2	94	1.7800	Molecule twist	IM9	100	13.5119	Molecule rock twist
TS2	561i	9.4787	C2–O stretch	TS12	1278i	478.1140	C1–H4–C2 asym. stretch
IM3	239	0.7169	Molecule rock o. p.	CH ₂ O	1201	4.7434	H–C–H rock o. p.
TS3	1204i	42.3824	C1–C2 stretch	CH ₃ CN	382	0.1699	Molecule ben
CH ₃ CHO	152	1.0732	Molecule twist	TS13	1529i	409.5485	N–H4 rock i. p.
HCN	766	42.3094	H–C–N bend	IM10	66	3.9620	Molecule twist
TS4	1575i	179.9820	C–H3 rock i. p.	TS14	211i	69.1377	C2–N stretch
IM4	146	1.1921	Molecule rock i. p.	IM11	139	2.7332	Molecule twist
TS5	389i	65.0909	N–O–C2 asym. stretch	TS15	204i	10.9783	C1–N stretch
IM5	186	8.9465	Molecule twist	CH ₃ CCH	343	10.5855	Molecule twist
TS6	357i	49.7411	N–H3&C1–C2 asym. stretch	HNO	1565	3.5890	H–N–O bend
IM6	33	2.8766	Molecule rock i. p.	TS16	373i	14.4964	C1–C2–N asym. stretch
HNC	807	165.9020	H–N–C bend	IM12	169	3.7375	Molecule rock i. p.
TS7	581i	301.0360	O–H3 rock i. p.	TS17	301i	26.2279	C–H3&C2–N asym. stretch
TS8	1884i	530.1020	O–H6 stretch	IM13	25	0.7861	Molecule rock i. p.

D. Formation of CH₂O+CH₃CN

The triatomic ring of IM5 can be breached through C2–O breakage and a new triatomic ring forms via TS9, forming IM7. In TS9, the breaking C2–O bond is extended to 0.2159 nm and the bond distance of the newly formed C2–N is 0.2452 nm. The imaginary frequency (661 i cm^{-1} , 62.8647 km/mol) is the C1–O–C2 stretch mode. The triatomic ring of IM7 will open through C1–C2 cleavage via TS10 to form IM8. Certainly this imaginary frequency is the C1–C2 stretch mode, which connects the two IMs. In IM8, C1, N, C2, and O atom are coplanar, the two single electrons on C1 and the lone-pair electrons can be delocalized to N and C2, forming a Π_4^0 bond and a bis(alkylidene) structure. Subsequently H3 shifts from O to C1 via the three-atom-ringed TS11, producing IM9. Then, via TS12, C1 attracts H4 from C2, the bond lengths of C1–H4 and C2–H4 are 0.1384 and 0.1436 nm, respectively; simultaneously the C1–N bond extends to 0.1844 nm, decomposing to formaldehyde CH₂O and acetonitrile CH₃CN. The energy barrier of this process is very high (298.17 kJ/mol), so it is the speed determining process of this channel.

E. IM1→CH₃CCH+HNO

The H4 atom of IM1 can also shift from C2 to N via TS13 with a four-membered ring, forming IM10. The

distances of the shifting H4 to C2 and N are 0.1594 and 0.1246 nm, respectively. The corresponding imaginary frequency is assigned to the N–H4 rock in plane mode (1529 i cm^{-1} , 409.5485 km/mol). Subsequently, N links to C2 via TS14, forming IM11 with a three-atom ring. For TS14, the newly formed C2–N bond distance is 0.1843 nm, and the imaginary frequency is its stretch mode at 211 i cm^{-1} . HNO then leaves C1 and C2 via TS15, forming propyne CH₃CCH and Hyponitrite acid HNO. The energy barrier from IM1 to IM10 is relatively high (247.52 kJ/mol), so this channel is unfavorable energetically.

IV. CONCLUSION

C₃H₅· has three isomers, allyl, 1-propenyl, and 2-propenyl, and is an ideal model for studying the intermolecular and intramolecular reactions of complex organic free radicals containing C=C double bonds. In this study, one isomer 1-propenyl was selected. The radical reaction system of 1-propenyl radical with NO was investigated extensively with the Gaussian 98 package at the B3LYP/6-311++G** level. Connections of the transition states and products were confirmed by IRC calculation. Using the relative energies after TC and ZVPE corrections, the potential energy surface was drawn. Subsequently, using vibrational mode analysis, the reaction mechanism was eluci-

dated. There are seven reaction pathways and five sets of small molecule end products, $\text{CH}_2\text{O}+\text{CH}_3\text{CN}$, $\text{CH}_2\text{CHCN}+\text{H}_2\text{O}$, $\text{CH}_3\text{CHO}+\text{HCN}$, $\text{CH}_3\text{CHO}+\text{HNC}$ and $\text{CH}_3\text{CCH}+\text{HNO}$. The PES shows that the channel of $\text{C}_3\text{H}_5\cdot+\text{NO}\rightarrow\text{IM1}\rightarrow\text{TS1}\rightarrow\text{IM2}\rightarrow\text{TS2}\rightarrow\text{IM3}\rightarrow\text{TS3}\rightarrow\text{CH}_3\text{CHO}+\text{HCN}$ is favorable thermodynamically, and the energies of all TSs are lower than that of $\text{C}_3\text{H}_5\cdot+\text{NO}$. The decomposition of IM5 can lead to a series of products; once IM1 is activated and the energy barrier of TS4 is surpassed, all these 5 channels are also competitive. By comparison, the channel of $\text{C}_3\text{H}_5\cdot+\text{NO}\rightarrow\text{IM1}\rightarrow\text{TS13}\rightarrow\text{IM10}\rightarrow\text{TS14}\rightarrow\text{IM11}\rightarrow\text{TS15}\rightarrow\text{CH}_3\text{CCH}+\text{HNO}$ is unfavorable energetically. This study also shows that, because of the structural undersaturation, the reactivity of organic free radicals containing C=C double bonds is very complicated, and they are apt to form ring structures in reaction processes, involving a series of structural transformation and isomerization processes to generate more stable species.

V. ACKNOWLEDGMENT

This work was supported by the National Natural Science Foundation of China (No.10674099).

- [1] R. F. Liu, T. T. Huang, J. Tittle, and D. H. Xia, *J. Phys. Chem. A* **104** 8368 (2000).
- [2] X. L. Cheng, Z. Y. Zhou, Y. Y. Zhao, Y. F. Sun, and Y. Zhu, *J. Mol. Struct. (THEOCHEM)* **725** 103 (2005).
- [3] M. Zhao, X. M. Pan, P. J. Liu, H. Sun, Z. M. Su, and R. S. Wang, *Chem. J. Chin. Univ.* **24**, 1648 (2003).
- [4] S. K. Wang, Q. Z. Zhang, J. H. Zhou, and Y. S. Gu, *Acta Chim. Sin.* **62**, 550 (2004).
- [5] Z. X. Zhang, G. Xu, L. S. Pei, C. X. Chen, and Y. Chen, *Chin. J. Chem. Phys.* **17**, 326 (2004).
- [6] P. J. Liu, X. M. Pan, M. Zhao, H. Sun, Z. M. Su, and R. S. Wang, *Chem. J. Chin. Univ.* **25**, 685 (2004).
- [7] G. L. Dai, Y. C. Wang, L. L. L., D. M. Wang, and Z. Y. Geng, *Acta Chim. Sin.* **63**, 703 (2005).
- [8] X. L. Yang, H. L. Wang, D. F. Zhao, Y. Chen, and C. X. Chen, *Chin. J. Chem. Phys.* **18**, 479 (2005).
- [9] R. Sumathi, D. Sengupta, and M. T. Nguyen, *J. Phys. Chem. A* **102**, 3175 (1998).
- [10] S. A. Kulkarni and N. Koga, *J. Phys. Chem. A* **102**, 5228 (1998).
- [11] M. Baer, H. R. Volpp, and J. Wolfrum, *J. Phys. Chem. A* **102**, 10455 (1998).
- [12] M. Weissman and S. W. Benson, *Prog. Energy Combust. Sci.* **15**, 273 (1989).
- [13] R. E. Linder, D. L. Winters, and A. C. Ling, *Can. J. Chem.* **54**, 1405 (1976).
- [14] J. A. Mueller, J. L. Miller, L. J. Butler, F. Qi, O. Sorkhabi, and A. G. Suits, *J. Phys. Chem. A* **104**, 11261 (2000).
- [15] F. A. Kong and F. Dong, *Chin. J. Chem. Phys.* **17**, 225 (2004).
- [16] H. Zhang, Y. H. Ding, Z. S. Li, *J. Mol. Struct. (THEOCHEM)* **9**, 764 (2006).
- [17] H. Zhang, Y. B. Sun, Z. S. Li, and C. C. Sun, *Chem. J. Chin. Univ.* **27**, 2390 (2006).
- [18] M. J. Frisch, G. W. Trucks, H. B. Schlegel, G. E. Scuseria, M. A. Robb, J. R. Cheeseman, V. G. Zakrzewski, J. A. Montgomery, Jr., R. E. Stratmann, J. C. Burant, S. Dapprich, J. M. Millam, A. D. Daniels, K. N. Kudin, M. C. Strain, O. Farkas, J. Tomasi, V. Barone, M. Cossi, R. Cammi, B. Mennucci, C. Pomelli, C. Adamo, S. Clifford, J. Ochterski, G. A. Petersson, P. Y. Ayala, Q. Cui, K. Morokuma, D. K. Malick, A. D. Rabuck, K. Raghavachari, J. B. Foresman, J. Cioslowski, J. V. Ortiz, B. B. Stefanov, G. Liu, A. Liashenko, P. Piskorz, I. Komaromi, R. Gomperts, R. L. Martin, D. J. Fox, T. Keith, M. A. Al-Laham, C. Y. Peng, A. Nanayakkara, C. Gonzalez, M. Challacombe, P. M. W. Gill, B. Johnson, W. Chen, M. W. Wong, J. L. Andres, C. Gonzalez, M. Head-Gordon, E. S. Replogle, and J. A. Pople, *Gaussian 98, Rev. A.3*, Pittsburgh, PA: Gaussian, Inc., (1998).
- [19] A. D. Becke, *J. Chem. Phys.* **98**, 5648 (1993).
- [20] C. Lee, W. Yang, and R. G. Parr, *Phys. Rev. B* **37**, 785 (1988).
- [21] K. Fukui, S. Kato, and H. Fujimoto, *J. Am. Chem. Soc.* **97**, 1 (1975).
- [22] K. Ishida, K. Morokuma, and A. Komornicki, *J. Chem. Phys.* **66**, 2153 (1977).
- [23] Z. Gonzalez, H. B. Schlegel, *J. Phys. Chem.* **90**, 2154 (1989).
- [24] X. L. Cheng, G. X. Li, Z. M. Wang, Y. Y. Zhao, and Y. F. Sun, *Chin. J. Chem. Phys.* **20**, 326 (2007).
- [25] X. L. Cheng, L. Niu, Y. Y. Zhao, and Z. Zhou, *Spectrochim. Acta A* **60**, 907 (2004).
- [26] X. L. Cheng, *J. Mol. Struct. (THEOCHEM)* **731**, 89 (2005).